J Neurooncol (2016) 128:21–28
DOI 10.1007/s11060-016-2088-y

LABORATORY INVESTIGATION

Cationizable lipid micelles as vehicles for intraarterial glioma treatment

Juliane Nguyen[1] · Johann R. N. Cooke[2] · Jason A. Ellis[3] · Michael Deci[1] · Charles W. Emala[2] · Jeffrey N. Bruce[3] · Irving J. Bigio[4,5] · Robert M. Straubinger[1,6] · Shailendra Joshi[2]

Received: 13 December 2015 / Accepted: 15 February 2016 / Published online: 22 February 2016

Abstract The relative abundance of anionic lipids on the surface of endothelia and on glioma cells suggests a workable strategy for selective drug delivery by utilizing cationic nanoparticles. Furthermore, the extracellular pH of gliomas is relatively acidic suggesting that tumor selectivity could be further enhanced if nanoparticles can be designed to cationize in such an environment. With these motivating hypotheses the objective of this study was to determine whether nanoparticulate (20 nm) micelles could be designed to improve their deposition within gliomas in an animal model. To test this, we performed intra-arterial injection of micelles labeled with an optically quantifiable dye. We observed significantly greater deposition (end-tissue concentration) of cationizable micelles as compared to non-ionizable micelles in the ipsilateral hemisphere of normal brains. More importantly, we noted enhanced deposition of cationizable as compared to non-ionizable micelles in glioma tissue as judged by semiquantitative fluorescence analysis. Micelles were generally able to penetrate to the core of the gliomas tested. Thus we conclude that cationizable micelles may be constructed as vehicles for facilitating glioma-selective delivery of compounds after intraarterial injection.

Keywords Blood–brain barrier · Brain tumor · Chemotherapy · Glioma · Nanoparticle

Introduction

Angiogenesis and cell proliferation, as occurs during glioma growth and progression, may result in compromise of the blood brain/tumor barrier (BBB). In such an environment, endothelial membranes and tumor cells have been shown to express an abundance of anionic lipids [1]. These anionic lipids result in increased negative charge on malignant cells as compared to normal cells [2–5]. The ability of cationic drugs and tracers to target malignant tissue due to their charge differential has diagnostic and therapeutic implications [6]. Furthermore, the pH within glioma interstitium is relatively acidic (as low as 6.4) compared to the normal interstitium, enabling ready chemical distinction between the two environments [7]. Thus, the delivery of nanoparticulate micelles that are functionalized with amine groups and that ionize in an acidic pH could enhance the selectivity of candidate intraarterial anti-glioma drugs.

Electronic supplementary material The online version of this article (doi:10.1007/s11060-016-2088-y) contains supplementary material, which is available to authorized users.

✉ Jason A. Ellis
jae2109@columbia.edu

Shailendra Joshi
sj121@cumc.columbia.edu

1 Department of Pharmaceutical Sciences, University at Buffalo, State University of New York, Buffalo, NY, USA

2 Department of Anesthesiology, College of Physicians and Surgeons, Columbia University, 630 West 168th Street, P&S Box 46, New York, NY 10032, USA

3 Department of Neurological Surgery, Columbia University, New York, NY, USA

4 Department of Electrical Engineering, Boston University, Boston, MA, USA

5 Department of Biomedical Engineering, Boston University, Boston, MA, USA

6 Department of Pharmacology & Therapeutics, Roswell Park Cancer Institute, Buffalo, NY, USA

Our technique of intraarterial (IA) drug delivery, which is performed during transient cerebral hypoperfusion (TCH), offers many advantages for delivering cationic or cationizable particles [8]. The IA-TCH method enables the delivery of drug/tracers in the arterial distribution [9]. For micellar vehicle delivery, this could be significantly advantageous. First, the IA-TCH method achieves considerably higher concentrations in the arterial blood at the site of injection. High concentrations of micelles in the brain at the site of glioma infiltration will facilitate diffusion across the compromised blood-tumor barrier. Upon contact with the endothelium, the low pH of environment will lead to cationization. At the same time, the IA-TCH method minimizes opsonization by decreasing contact between micelles and anionic blood proteins and cells. Additionally, this method of delivery decreases shear stress on the micelles while facilitating electrostatic interactions by increasing the duration of contact between the micelles and the vascular endothelium/glioma cell membrane [10]. We therefore hypothesize that cationizable micelles, when injected using the IA-TCH method, will be an effective means of delivery to brain gliomas.

We have previously reported that significant improvements in the regional delivery of 80–200 nm cationic liposomes were achieved using the IA-TCH method [11]. However, particle delivery was variable and occasionally limited in larger tumors [10]. Therefore, in the work presented here, we have investigated the feasibility of using smaller (20 nm) micellar vehicles for achieving selective targeting of glioma implants. Specifically, we compared the delivery of cationizable and non-ionizable micelles loaded with the fluorescent DiD 680 dye. This enabled measurement of micellar concentrations and distribution by both quantitative and semi-quantitative optical methods.

Methods

Preparation of micelles

The micellar carriers were prepared as described previously [12]. Briefly, DSPE-mPEG(2000) or DSPE-PEG(2000)-amine (Avanti Polar Lipids) (Supplementary Fig. 1) were mixed with 1,1′-dioctadecyl-3,3,3′,3′ tetramethylindodi-carbocyanine, 4-Chlorobenzene-sulfonate Salt) at a molar ratio of 98/2. The pegylated lipid mixture was then dried down in a glass tube to a thin PEG-lipid film using a rotary evaporator. The lipid film was rehydrated in phosphate buffered saline (PBS) and sonicated for 10 min at room temperature until all components were dispersed. The particle sizes of the cationizable, amine-functionalized micelles DSPE-PEG(2000)-amine and methoxy-PEG–DSPE (mPEG–DSPE were measured by dynamic light scattering (DLS) using the Nanobrook Omni (Brookhaven). To determine the effect of pH on zeta potential, the micelles were dispersed in PBS at pH 7.4 and in 20 mM of 2-(*N*-morpholino) ethanesulfonic acid (MES) buffer at pH 6.5, 6.0, and 5.5 [13]. Measurements were taken three times per sample and are represented as mean ± SD.

In vitro spectroscopic analysis

DiD loaded micelles were dissolved in 10 % intralipid. The dissolved concentrations were compared to concentrations measured by diffuse reflectance spectroscopy (DRS) and semi-quantitative fluorescence imaging [14–17]. We used a custom built device for DRS measurements (Optimum Technologies Inc. Boston, MA) that employs a Xe light source to generate white light (450–850 nm). The light is delivered to the target site via a fiberoptic cable. The backscattered light is relayed to a spectroscope back via another cable. Spectral analysis of the returning light is used to determine tracer and drug concentrations. For semi-quantitative fluorescence imaging, we used 635 ± 5 nm LED light excitation and imaged through a 680 ± 5 nm band-pass filter using an electron multiplying charge-coupled device (emCCD, Evolve 512, Photometrics Inc.). The camera corrects for background noise and can quantify the photon yield.

The dissolved concentrations were compared to concentrations measured by diffuse reflectance spectroscopy (DRS) and semi-quantitative fluorescence imaging. Both diffuse reflectance spectroscopy and fluorescence measurements correlated well with the dissolved micelle concentrations (Fig. 1).

In vivo studies

Institutional Review Board (IRB) and Animal Care and Use Committee approval was obtained for all studies. In vivo experiments were conducted on two groups of animals: 1. Group 1 consisted of healthy Sprague–Dawley rats (n = 10) and 2. Group 2 consisted of Fisher 344 rats harboring implanted 9L-gliomas (n = 10). Surgical procedures were carried out under general ketamine and isoflurane anesthesia. Tail vein line, tracheostomy, and right common carotid catheter was placed, followed by ligation of all the branches of the external carotid artery. The DRS probe was placed over the right parietal region in Group 1 and close to the site of tumor implantation in Group 2. The laser Doppler probe to monitor cerebral blood flow (CBF) was placed just in front of the bregma over the right frontal region. In addition, we monitored the inspired and exhaled gas composition, skin blood flow, EKG, pulse oxygen saturation and volume and rectal

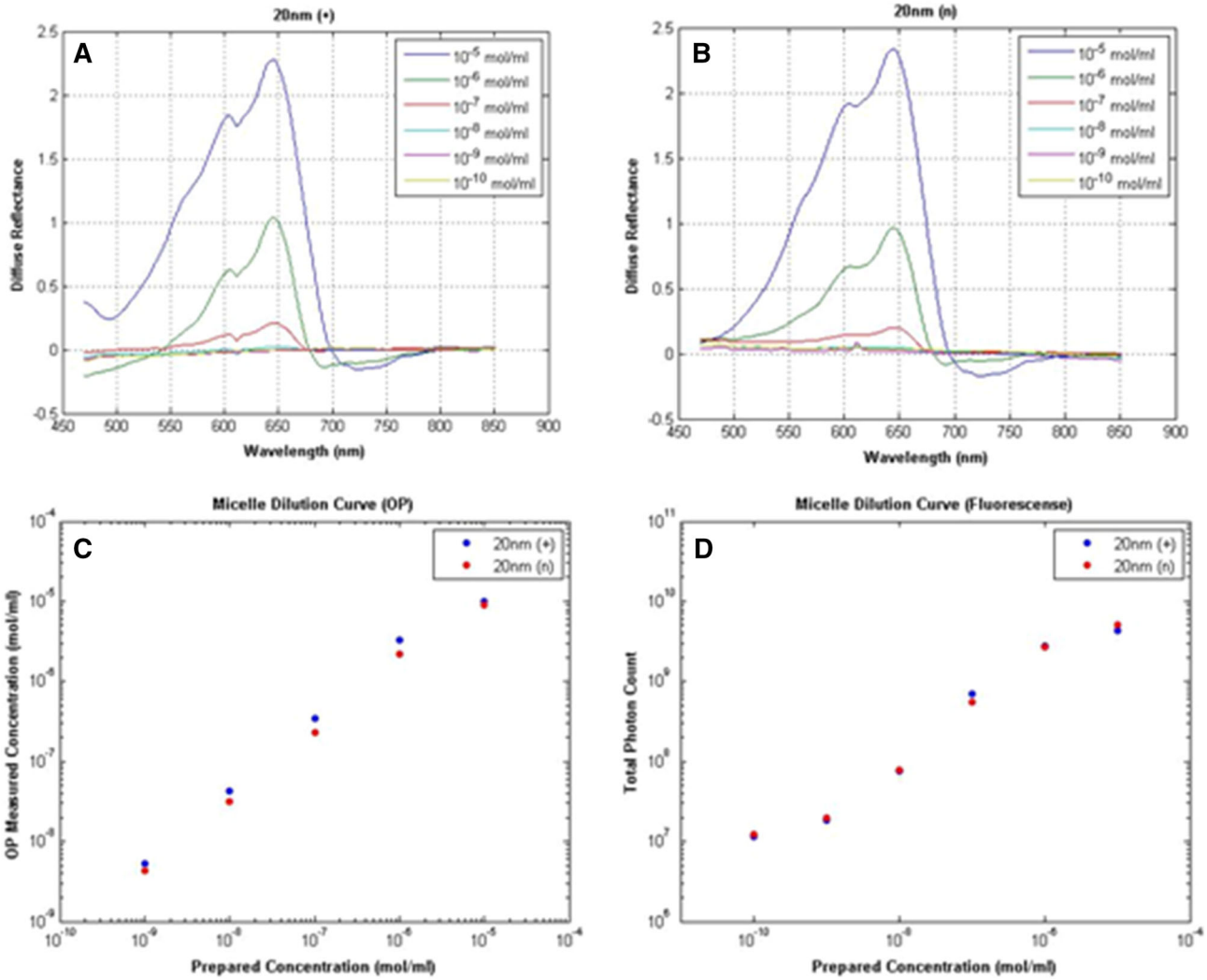

Fig. 1 In vitro characterization of micelles. Diffuse reflectance spectra of serially diluted cationizable (**a**) and non-ionizable (**b**) micelles are shown. Correlation plots comparing prepared micelle concentrations to measured concentrations by diffuse reflectance spectroscopy (**c**) and fluorescence are also show (D)

temperature. All physiological data was recorded in real-time by Mac Lab software (AD instrument, Boston MA). DRS measurements were recorded over a period of approximately 30 min. The first twelve baseline measurements were made over 1 min. Next, 300 measurements were taken 500 ms apart. The last 300 measurements were undertaken 5000 ms apart. Thus changes in tissue tracer concentrations with each micelle injection were tracked for approximately 30 min (end-concentration).

We injected IA drugs using a pneumatically driven 1 ml syringe with a Parker III injector controlled by an Aligent II Signal generator (Applied Signal Inc.). Hypotension was induced by administering a bolus intravenous injection of adenosine (2–3 mg), esmolol (2–3 mg), and cold saline (4° C, 1.5 ml). Pulsed intracarotid injections (60–70 µl) were delivered every 2 s such that micelles were injected within 30 s of the peak of hypotension (Fig. 2).

Rodent gliosarcoma cells (9L) were cultured to confluence in T25 flasks in Dulbecco's modified Eagle's medium (DMEM) with 10 % fetal bovine serum, penicillin/streptomycin, and kept humidified at 37 °C with 5 % CO_2. On the day of implantation in Group 2 animals, cells were trypsinized, washed, and resuspended to $4X10^5$ cells (85–95 % viability) in 5 µl of basal DMEM. Stereotactic implantation was performed using a 33-G Hamilton needle at a location 2 mm posterior, 3 mm lateral, and 3.5 mm deep to bregma over the right hemisphere. Tumors were allowed to grow for 16–18 days post implantation prior to commencing intraarterial delivery experiments. All animals remained asymptomatic at the time of intraarterial delivery.

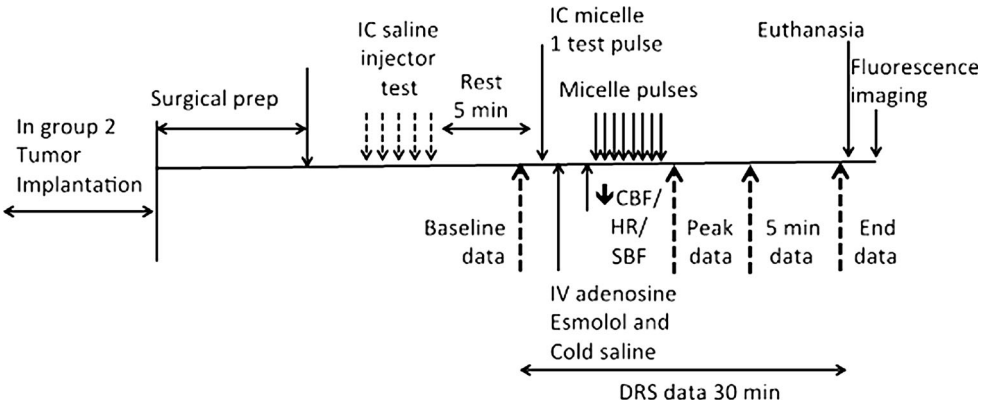

Fig. 2 In vivo experimental protocol

Micelle characterization

The size of micelles were determined by dynamic light scattering. Micelles composed of PEG-lipid functionalized with a primary amine displayed a hydrodynamic diameter of 18.76 ± 4.78 nm and the micelles composed of PEG-lipid containing non-ionizable methoxy groups displayed a hydrodynamic diameter of 21.46 ± 2.98 nm. Zeta potential measurements were used to characterize the pH-dependent surface charge of the cationizable micelles. For the cationizable micelles we observed a pH-dependent increase in the zeta potential values (Suppl. Table 1). At physiological pH, the cationizable micelles were neutral. As the pH was decreased to 6.5, 6.0, and 5.5 the zeta potential became positive, increasing to 6.1 mV ± 2.1, 9.2 mV ± 3.8, and 10.1 mV ± 2.8, respectively. For the non-ionizable micelles the zeta potential was slightly negatively charged at pH 7.4 (−5.9 mV ± 1.7). No significant changes in zeta potential were observed with a decrease in pH.

Data analysis

Pharmacokinetic analyses included peak and end concentrations of the dye and the area under the concentration time curve (AUC). Hemodynamic data was analyzed at baseline, at the peak of hypotension after micelle injection, 5 min after micelle delivery, and at the end of the experiment prior to euthanasia. Statistical analysis was done with repeated measures and factorial ANOVA with use of the Bonferroni Dunn test for post hoc correction. Significance was set at $p < 0.05$.

Results

Physiological changes during intraarterial injection

Heart rate and skin blood flow changes were similar in both Group 1 and Group 2 animals. It is notable that during transient cerebral hypoperfusion, the cerebral blood flow reduction was marked with a more rapid recovery of animals treated with non-ionizable micelles (Fig. 3).

Intraarterial micellar delivery to Group 1

Peak ipsilateral hemispheric concentrations showed a trend toward being highest for cationizable as compared to non-ionizable micelles (2.2 ± 1.0 μM versus 1.3 ± 0.3 μM) but the difference did not meet statistical significance. Similarly the area under the concentration–time curve was 241 ± 71 μM s for cationizable versus 148 ± 71 μM s for non-ionizable micelles delivery, but this difference was not significant ($p = 0.07$). On the other hand, the end-tissue dye concentration were significantly different with concentrations of 3.4 ± 0.03 versus 1.7 ± 0.1 μM for the cationizable and non-ionizable micelle delivery respectively ($p < 0.01$). Semi-quantitative fluorescence imaging revealed weak signals indicative of uptake of both micelle types, although cationizable and non-ionizable micelles were clearly evident in larger veins and some arteries.

Intraarterial micellar delivery to Group 2

In vivo DRS in live animals revealed no significant differences in the tissue concentrations measured for the two micelle formulations: peak dye concentration was 1.05 ± 0.70 versus 0.99 ± 0.67 μM, end concentration was 0.41 ± 0.23 versus 0.21 ± 0.21 μM, and the area under the curve was 250 ± 122 versus 146 ± 100 μM s for the groups administered cationizable micelles versus non-ionizable micelles, respectively. However, postmortem fluorescence imaging revealed much higher signals indicative of micelle deposition within tumors targeted by cationizable micelles as compared to non-ionizable micelles (Figs. 4 and 5).

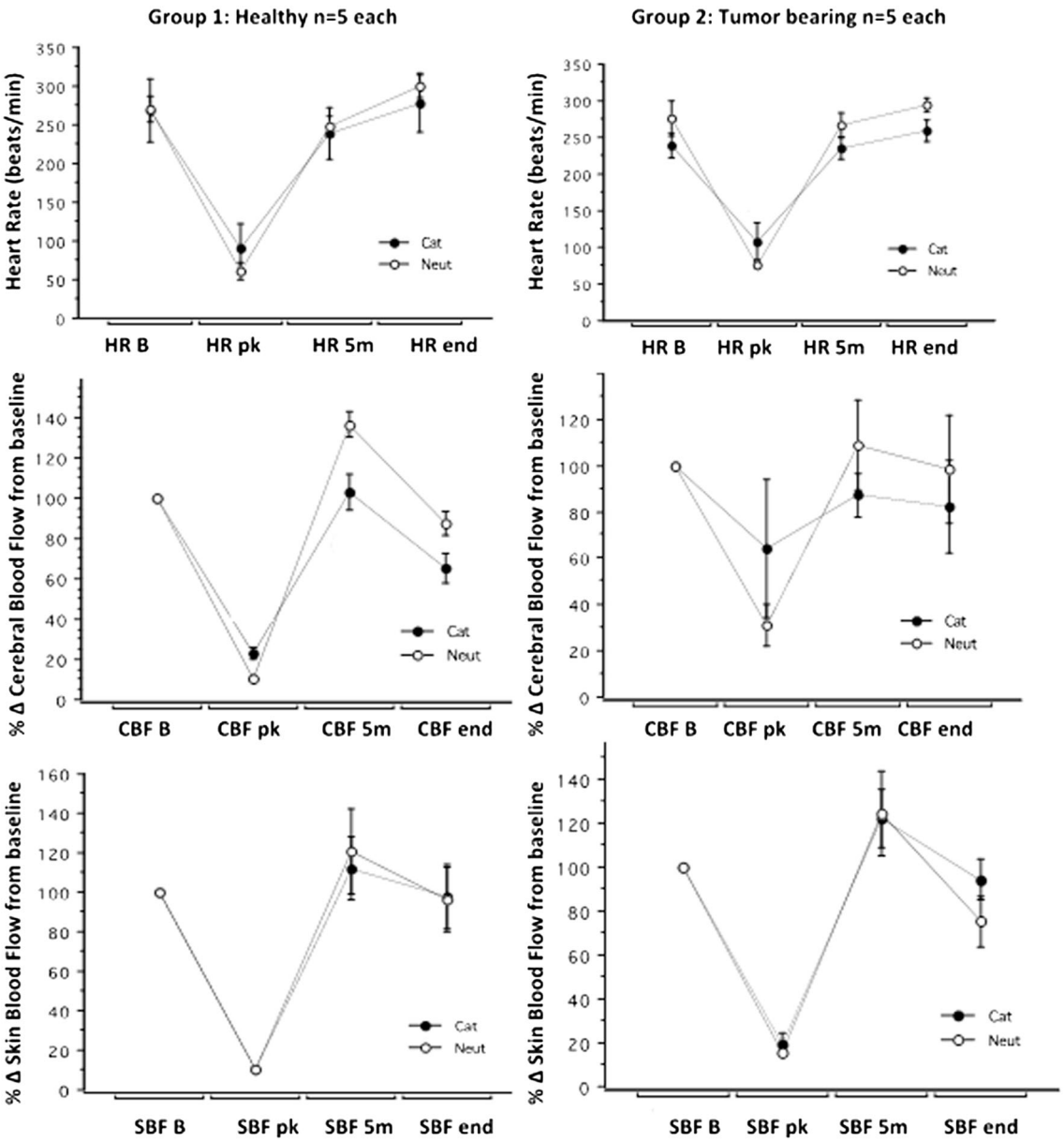

Fig. 3 Physiological changes during IA-TCH. Changes in heart rate, cerebral blood flow, and skin blood flow in healthy (*left*) and tumor bearing rats (*right*) are shown

Discussion

In vivo quantitative spectroscopy (DRS) indicate a trend toward greater brain and glioma uptake of cationizable versus non-ionizable micelles. Semi-quantitative, post-mortem fluorescence analysis (computer generated visual fluorescence maps) suggests a more dramatic preference of cationizable micelles for deposition within gliomas. Although quantitative experiments did not always meet statistical significance, we are encouraged by these findings that, at least qualitatively, corroborate our mechanistic understanding of charged liposome-tissue interactions. Indeed the failure of DRS to quantitatively confirm the seemingly overwhelming preference of cationic micelles for gliomas seen in post mortem fluorescence images may be a consequence of limitations to the DRS technique itself. DRS measures signal from a small volume of tissue which may not be sufficient to accurately sample the entire volume of larger tumors [18]. Thus upon inspection of the complete set of raw fluorescence images (Figs. 4 and 5) we conclude that cationizable micelles preferentially target the model gliomas used in our studies.

We observed two major differences in IA-TCH delivery of micellar formulations compared to our previous observations on liposomal delivery. First, as depicted in Fig. 4,

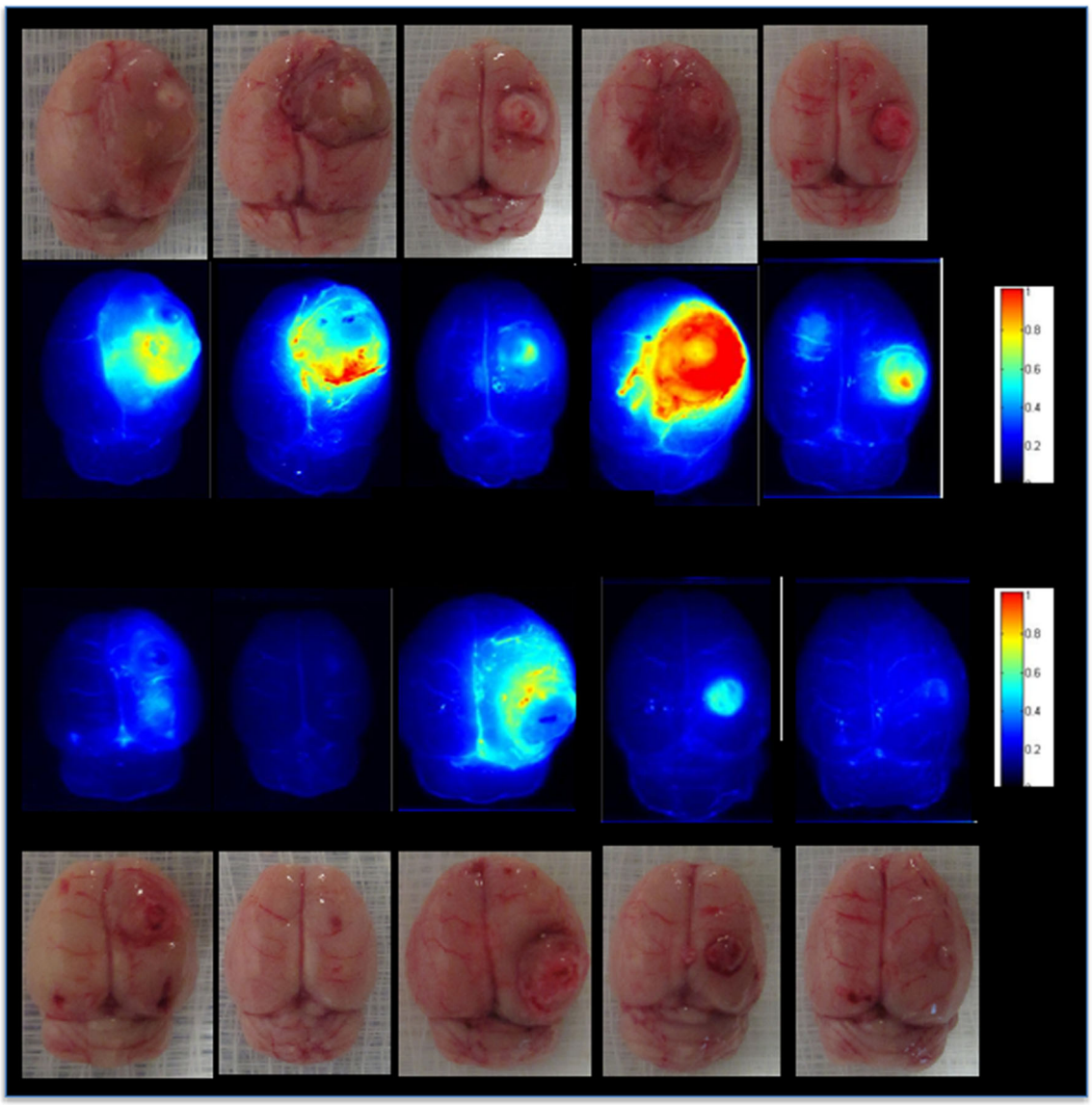

Fig. 4 Post mortem fluorescence analysis of uncut brains. Photographs of gross glioma-bearing brains and corresponding fluorescence images after IA-TCH delivery are shown. Cationizable micelles delivery clearly results in significant tumor-localizable, fluorescence signals (*top two rows*). Less robust tumor-localizable, fluorescence signals are observed after non-ionizable micelles are delivered to animals (*bottom two rows*)

cortical vessels are clearly evident in post mortem specimens of rats that were administered either micellar preparations; we rarely observed such a pattern of vascular deposition with conventional liposomes in previous studies [8, 10, 19]. Second, we observed that both micelle formulations were able to undergo deposition within large tumors, although the cationizable micelles appeared to be more effective. However, cross sectional imaging revealed their distribution within the lesion was heterogeneous. We suspect that the variability of deposition results from the structural variability within the lesion, and subtle differences in the arterial supply, blood flow, and pH. Thus, variability in micelle deposition within large tumors is to be expected.

This study suggests that the optimization of drug vehicle formulations can have a significant impact on IA drug delivery. A general perception that IA drug delivery has failed to achieve the benefits anticipated is fundamentally flawed. IA chemotherapy now has an established role in the treatment of retinoblastomas and advanced liver cancers [20]. What makes IA glioma treatment clinically challenging is general nihilism due to failure of all other approaches to treat this disease combined with the risk of neurological injury upon administration. The dismal outcome of treatment for glioma provides an incentive to seek better methods of tumor-selective drug delivery. Several clinical trials investigating IA drug delivery are currently

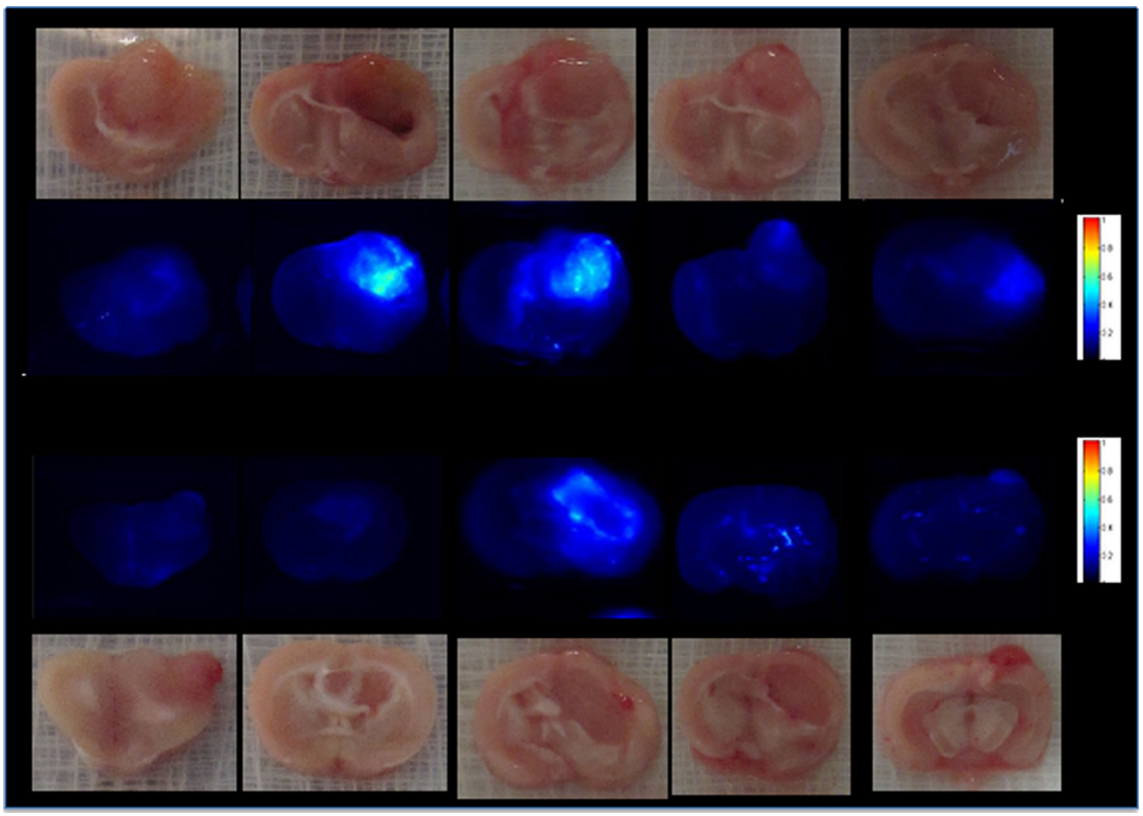

Fig. 5 Post mortem fluorescence analysis of sectioned brains. Photographs and fluorescence images of brain sections (corresponding to whole brain images in Fig. 4) after IA-TCH delivery of cationizable micelles (*top two rows*) and non-ionizable micelles (*bottom two rows*) are shown. The overall distribution and tumor core penetration of cationizable micelles is variable but clearly more robust than for non-ionizable micelles

ongoing. These trials are largely focused on the safety of IA chemotherapy. However, the risks/benefits of IA treatments will change dramatically if the drug can target tumors selectively.

The key to effective IA drug delivery is the rapid uptake of the drugs and nanoparticles during their first pass through the cerebral circulation. However, the majority of drugs screened thus far are seldom formulated to provide rapid regional uptake after IA administration. Furthermore, precise optimization of injection parameters, including concurrent manipulation of blood flow, has not been attempted. Even in preclinical research, Hardebo recognized the significance of the IA bolus volume, but the concepts were seldom applied to improve drug delivery. For rats he recommended a 10 µl injection volume [21]. In the present study, we used a volume of 65 µl/pulse, based on our measurements using optical coherence tomography [10]. This pulse volume was sufficient to displace blood in the arterial dead space without spilling over to the venous side. The combination of optimized drug delivery formulations, careful selection of injection parameters and concurrent manipulation of blood flow represent a significant shift from the IA treatment paradigms of the past.

The combination of tumor targeting strategies with the IA-TCH method of drug delivery can be highly synergistic for cationic and cationizable drugs. During IA-TCH injections, the injection of the drug momentarily displaces the blood downstream of the injection. Consequently, non-specific opsonization of drug formulations by blood components that carry an anionic charge is minimized or even avoided. By using cationizable micellar carriers that are neutral at physiological pH but become cationic in the acidic microenvironment of the gliomas, we are able to: (1) minimize undesired interactions with blood components at pH 7.4 and (2) increase in vivo biocompatibility. The pH in gliomas have been reported to be as low as 6.4, with a mean of 6.8 [7, 22]. As a tumor's mass increases, pH tends to become more acidic but also more variable [22, 23]. As shown by our zeta potential measurements, cationizable lipids become positively charged with decreasing pH. This most likely contributes to the significantly enhanced deposition and retention of the cationizable micelles in the gliomas compared to the non-ionizable PEG–DSPE micelles. In addition, because of the reduction in blood flow, the transit time through the cerebral circulations is drastically increased and shear stress on the particles is

greatly decreased. As a result, there is considerable improvement in drug/tracer delivery to and uptake by the vascular endothelium. To that end, the relative overexpression of anionic lipids on the surfaces of the epithelial and neoplastic cells can account for the tumor selectivity observed in our experiments.

Conclusion

Cationizable micelles appear to be superior to non-ionizable micelles for regional targeting of brain gliomas in the animal model tested. Additional studies are needed to quantitatively confirm these findings. Development of nanoparticulate cationizable micelles as drug delivery vehicles for glioma treatment may be a promising avenue for further investigation.

Funding National Cancer Institute at the National Institutes of Health RO1-CA-138643.

References

1. Janmey PA, Kinnunen PK (2006) Biophysical properties of lipids and dynamic membranes. Trends Cell Biol 16(10):538–546. doi:10.1016/j.tcb.2006.08.009
2. Marquez M, Nilsson S, Lennartsson L, Liu Z, Tammela T, Raitanen M, Holmberg AR (2004) Charge-dependent targeting: results in six tumor cell lines. Anticancer Res 24(3a):1347–1351
3. Abercrombie M, Ambrose EJ (1962) The surface properties of cancer cells: a review. Cancer Res 22:525–548
4. Dobrzynska I, Skrzydlewska E, Figaszewski ZA (2013) Changes in electric properties of human breast cancer cells. J Membr Biol 246(2):161–166. doi:10.1007/s00232-012-9516-5
5. Dobrzynska I, Szachowicz-Petelska B, Darewicz B, Figaszewski ZA (2015) Characterization of human bladder cell membrane during cancer transformation. J Membr Biol 248(2):301–307. doi:10.1007/s00232-015-9770-4
6. Jo DH, Kim JH, Lee TG, Kim JH (2015) Size, surface charge, and shape determine therapeutic effects of nanoparticles on brain and retinal diseases. Nanomed Nanotechnol Biol Med 11(7):1603–1611. doi:10.1016/j.nano.2015.04.015
7. Garcia-Martin ML, Martinez GV, Raghunand N, Sherry AD, Zhang S, Gillies RJ (2006) High resolution pH(e) imaging of rat glioma using pH-dependent relaxivity. Magn Reson Med 55(2):309–315. doi:10.1002/mrm.20773
8. Joshi S, Singh-Moon RP, Wang M, Chaudhuri DB, Holcomb M, Straubinger NL, Bruce JN, Bigio IJ, Straubinger RM (2014) Transient cerebral hypoperfusion assisted intraarterial cationic liposome delivery to brain tissue. J Neurooncol 118(1):73–82. doi:10.1007/s11060-014-1421-6
9. Joshi S, Wang M, Etu JJ, Suckow RF, Cooper TB, Feinmark SJ, Bruce JN, Fine RL (2008) Transient cerebral hypoperfusion enhances intraarterial carmustine deposition into brain tissue. J Neurooncol 86(2):123–132. doi:10.1007/s11060-007-9450-z
10. Joshi S, Singh-Moon RP, Ellis JA, Chaudhuri DB, Wang M, Reif R, Bruce JN, Bigio IJ, Straubinger RM (2015) Cerebral hypoperfusion-assisted intra-arterial deposition of liposomes in normal and glioma-bearing rats. Neurosurgery 76(1):92–100. doi:10.1227/NEU.0000000000000552
11. Joshi S, Singh-Moon R, Wang M, Chaudhuri DB, Ellis JA, Bruce JN, Bigio IJ, Straubinger RM (2014) Cationic surface charge enhances early regional deposition of liposomes after intracarotid injection. J Neurooncol 120(3):489–497. doi:10.1007/s11060-014-1584-1
12. Nguyen J, Sievers R, Motion JPM, Kivimae S, Fang QZ, Lee RJ (2015) Delivery of lipid micelles into infarcted myocardium using a lipid-linked matrix metalloproteinase targeting peptide. Mol Pharmaceut 12(4):1150–1157. doi:10.1021/mp500653y
13. Walsh CL, Nguyen J, Szoka FC (2012) Synthesis and characterization of novel zwitterionic lipids with pH-responsive biophysical properties. Chem Commun 48(45):5575–5577. doi:10.1039/c2cc31710a
14. Bigio IJ, Bown SG (2004) Spectroscopic sensing of cancer and cancer therapy: current status of translational research. Cancer Biol Ther 3(3):259–267
15. Mourant JR, Johnson TM, Los G, Bigio IJ (1999) Non-invasive measurement of chemotherapy drug concentrations in tissue: preliminary demonstrations of in vivo measurements. Phys Med Biol 44(5):1397–1417
16. Reif R, Wang M, Joshi S, A'Amar O, Bigio IJ (2007) Optical method for real-time monitoring of drug concentrations facilitates the development of novel methods for drug delivery to brain tissue. J Biomed Opt 12(3):034036
17. Ergin A, Wang M, Zhang J, Bigio I, Joshi S (2012) Noninvasive in vivo optical assessment of blood brain barrier permeability and brain tissue drug deposition in rabbits. J Biomed Opt 17(5):057008
18. Mourant JR, Bigio IJ, Jack DA, Johnson TM, Miller HD (1997) Measuring absorption coefficients in small volumes of highly scattering media: source-detector separations for which path lengths do not depend on scattering properties. Appl Opt 36(22):5655–5661
19. Joshi S, Singh-Moon R, Wang M, Chaudhuri DB, Ellis JA, Bruce JN, Bigio IJ, Straubinger RM (2014) Cationic surface charge enhances early regional deposition of liposomes after intracarotid injection. J Neurooncol. doi:10.1007/s11060-014-1584-1
20. Joshi S, Ellis JA, Ornstein E, Bruce JN (2015) Intraarterial drug delivery for glioblastoma mutiforme: will the phoenix rise again? J Neurooncol 124(3):333–343. doi:10.1007/s11060-015-1846-6
21. Hardebo JE, Nilsson B (1979) Estimation of cerebral extraction of circulating compounds by the brain uptake index method: influence of circulation time, volume injection, and cerebral blood flow. Acta Physiol Scand 107(2):153–159
22. Vaupel P, Kallinowski F, Okunieff P (1989) Blood flow, oxygen and nutrient supply, and metabolic microenvironment of human tumors: a review. Cancer Res 49(23):6449–6465
23. Kallinowski F, Vaupel P (1988) pH distributions in spontaneous and isotransplanted rat tumours. Br J Cancer 58(3):314–321